2022 IMEKO TC-4 International Conference on
Metrology for Archaeology and Cultural Heritage
University of Calabria, Italy, October 19-21, 2022

Rare Japanese fabrics of the Ragusa-Kiyohara collection. A spectroscopic characterization

Paola Marzullo[1,*], Lucia Nucci[2], Elena Piacenza[1,*], Federica Arcidiacono[1], Delia Francesca Chillura Martino[1]

[1] *Department of Biological, Chemical and Pharmaceutical Sciences and Technologies (STEBICEF), University of Palermo, Palermo, Italy,*
paola.marzullo@unipa.it; elena.piacenza@unipa.it; federica.arcidiacono@unipa.it; delia.chilluramartino@unipa.it
[2] *Regional direction Museums of Tuscany - Uffizi Galleries, Firenze, Italy,*
lucia.nucci@cultura.gov.it
**corresponding authors*

***Abstract* – The Vincenzo Ragusa and O'Tama Kiyohara artefact collection belonging to the Liceo Artistico Ragusa Kiyohara in Palermo is one outstanding example of the artistic encounter between the European and Eastern worlds.**
In this contribution, we report a physical-chemical characterization of Japanese fabrics of the Ragusa-Kiyohara collection. Metallic threads finely decorate these fabrics conferring their preciousness.
The X-ray fluorescence (XRF) analysis and the Attenuated total reflectance-Fourier transform infrared (ATR-FTIR) spectroscopy were used as complementary techniques for elemental identification and molecular recognition.
The artefacts presented here are a rare testimony of oriental art in our cultural heritage. Therefore, this work can be part of a path that, starting from the preliminary material knowledge, can develop appropriate restoration and conservation strategies.

I. INTRODUCTION

Japanese textile culture began in the Yamato period (300-710 A.D.) when nobility and the upper class increased the demand for delicate fabrics such as silk. The latter was used to create luxurious kimonos, a distinctive dress of oriental countries, but they are just one form of textile production. The existence of numerous social classes profoundly influenced the development of textile art in Japan. Japanese peasants wore hemp clothes made of hand-spun vegetable fiber. During the Muromachi period (1338-1477 A.D.), there was an increase in trade with the introduction of new materials and techniques. Indeed, the Japanese began importing cotton from China until the 16th century, when domestic cotton production grew significantly.
Cotton fibers replaced the use of hemp in textiles used by commoners. Between mid-18th and mid-19th cent., a textile art associated with the rural population, called folk, developed. Several of these fabrics became fascinating art objects for Janophile collectors [1].
Japanese art experienced a rare encounter with Europe for a long time until 1854. Indeed, two centuries of national seclusion isolated Japan from the outside world. Once it opened to western countries, numerous foreign experts and scientists were invited to contribute to the country's cultural and technological development [2].
The Italian sculptor Vittorio Ragusa travelled to Japan during the last decades of the 19th century. During his trip, the love story with O'Tama Kiyohara, a passionate painter, was decisive. The young woman left Japan to follow the sculptor to Palermo, where they married. O'Tama was one of the first Asian artists to come to Italy. She was innovative by breaking the classical schemes and making oriental art known in the Italian panorama [3]. Coming back from Japan, Otama and Ragusa brought Italy a rich and precious collection of objects belonging to the Japanese culture.
Unique Kinkarakawa-gami wallpapers belonging to the Vincenzo Ragusa and O'Tama Kiyohara Collection of Palermo (inheritance of the Liceo Artistico founded in the XIX century by the sculptor Vincenzo Ragusa) were the object of a combined physical-chemical and microbiological approach in our previous work [4].
The fabrics presented here are part of the same collection and are incredibly precious due to their limited presence in Europe. Besides the delicacy of yearn, the fabrics are enriched with metallic laminae and threads, producing iridescence and beautiful motifs. At the same time, their peculiarity makes them very delicate. Thus, a physical-chemical study is paramount to delineate a successful restoration approach. Fabrics were analyzed through non-invasive and non-destructive analytical methods that exclude any movement into a laboratory and prevent any sampling when possibile. The elemental study was performed by X-ray fluorescence spectroscopy. As a fast and non-destructive method, XRF has recently proven

versatile for cultural heritage studies [5],[6]. Among the molecular spectroscopy techniques, Attenuated total reflectance-Fourier transform infrared spectroscopy (ATR-FTIR spectroscopy) has been considered, as it requires a tiny amount and minimal sample preparation, permits routine analysis and is easy to operate.

II. EXPERIMENTAL SECTION

The studied fabrics belong to the Vittorio Ragusa-O'Tama Kiyohara collection of Palermo (Liceo Artistico Ragusa-Kyohara, Palermo, Italy). Analyzed samples are identified by inventory numbers (INV251, INV253 A-F, and INV254 A-F). XRF spectra were registered in sampling points characterized by different colors, while the ATR-FTIR analysis was carried out on weft, warp, or selvedge threads.

The XRF spectra were acquired by Tracer III SD Bruker AXS portable spectrometer (Bruker, UK) equipped with a Rhodium Target X-ray tube operating at 40 kV and 11 µA and a silicon drift X-Flash SDD with Peltier cooling system and 3-4 diameter spot as a detector. The X-ray emission peak of each element was integrated and reported in terms of net area to evaluate elements and their abundance.

ATR-FTIR spectra were recorded by using a µFTIR Lumos (Bruker, UK) equipped with a Platinum ATR and an IR microscope featuring 0.1 µm as lateral resolution. Spectra were collected in the 4000–600 cm^{-1} range, with a resolution of 2 cm^{-1} and 60 scans per sampling point, and were subsequently analyzed through OriginPro® 2016 software.

III. RESULTS AND DISCUSSION

X-ray fluorescence spectroscopy was considered a powerful tool to probe different patterns and colors to identify fabrics' composition and peculiar features. The lack of knowledge about the technology used for producing these textiles, the raw materials, and their processing prevented the possibility of building appropriate standards required to perform an accurate quantitative analysis. Moreover, the computation of concentration based on basic equations [7] and matrix effect correction [8] is challenging and far beyond the aim of the work. As a consequence, the spectra interpretation has been purely qualitative.

For representative purposes, we report the results of XRF analysis on the fabric named INV 251 (Figure 1a, b).

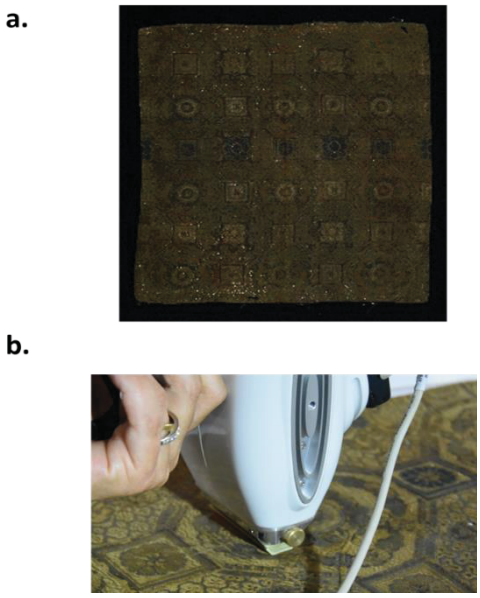

*Fig.1. INV 251 fabric **(a)**; acquisition of XRF spectra in a point of gold color **(b)**.*

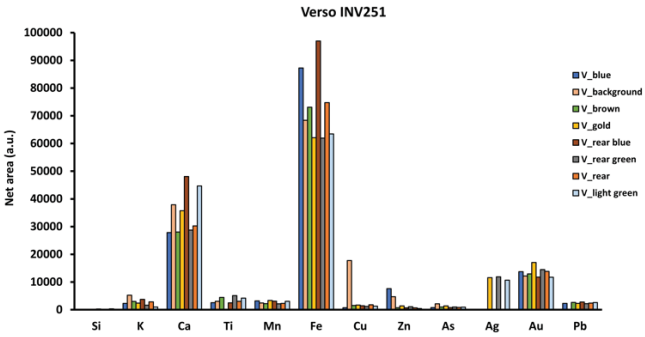

Fig.2. Elemental distribution determined by XRF analysis on Verso INV251.

In all analyzed textiles, ubiquitous elements are calcium, iron, manganese, and copper, which may have been introduced during the manufacturing process. Specifically, calcium (Ca) and iron (Fe) identified the highest fluorescence emission, thus suggesting their presence as the majority elements among the detectable ones in the experimental conditions. The lower intensity detected for potassium (K) and titanium (Ti) indicates that they could be considered minority elements compared to Ca. Similar considerations apply to manganese (Mn) and silver (Ag) in contrast to Fe. Additionally, L-lines for gold (Au) and lead (Pb) could not be directly compared to the K-lines for all other elements. Due to the high intensity of Au emission, it is reasonable to assume its presence as a majority element in the investigated sample, whereas lead is a minority element. Traces of silicon (Si), copper (Cu), zinc (Zn), and arsenic (As) were also observed. Point-to-point variation of the peak area for elements such as K, Ti, Au,

Pb, zinc (Zn), arsenic (As), and strontium (Sr) could indicate the use of various pigments for coloring (Table 1).

Table 1. Characteristic elements of sampling colors in the fabrics.

Color	Ubiquitous elements
Green	K, Ti, Zn, As, Au
Blue	Zn, As, Pb
Gold	K, Zn, As, Au, Pb
Beige	K, Zn, As, Sr, Pb
Brown	K, Ti, Zn, As, Pb

.

Nevertheless, the eventual presence of organic dyes could not be excluded on the basis of XRF findings. Thus, the above analysis was complemented by ATR-FTIR spectroscopy.

The ATR-FTIR spectra were acquired on single wires sampled from each fabric; Figure 3 reports spectra recorded on two wires of INV251 as an example.

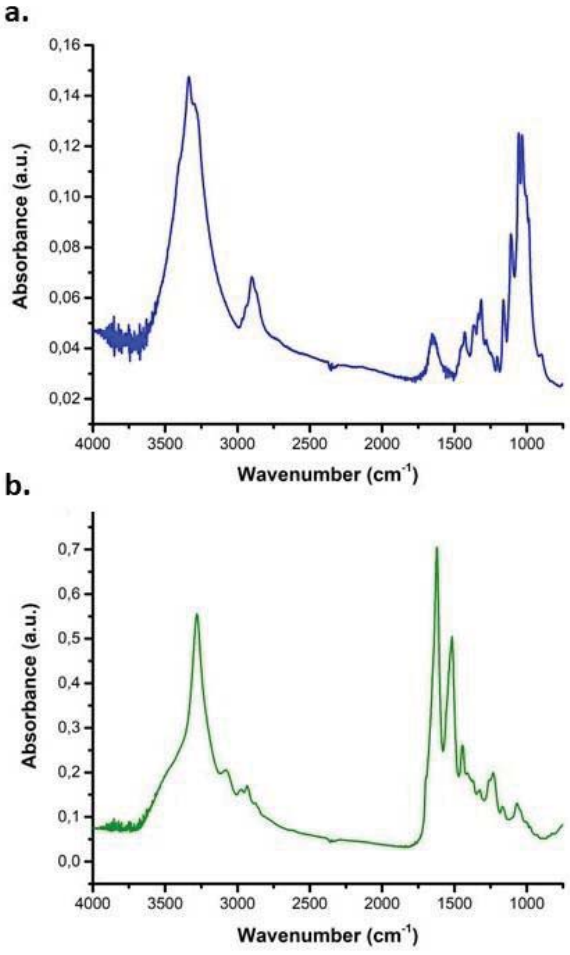

*Fig. 3. ATR-FTIR spectra of the sample warp lining 5A **(a)** and the sample light green warp **(b)** of INV 251.*

The two spectra are profoundly different and indicate cellulosic (Figure 3a) and proteinaceous material (Figure 3b).

The spectrum in figure 3a shows peaks attributable to the stretching of -OH groups involved in intermolecular (broad signal centered at 3346 cm^{-1}) or intramolecular (shoulder around 3300 cm^{-1}) hydrogen bonds characteristic of cellulose fibers. The band centered at 2910 cm^{-1} is the envelope of symmetric and antisymmetric -C-H stretching in $-CH_2$ and $-CH_3$ moieties and is typical of polymer chains, whereas the -OH bending at 1647 cm^{-1} is due to adsorbed water. The spectral region between 1500 cm^{-1} and 1200 cm^{-1} shows bending vibrational modes of $-CH_2$, -CH and -OH groups. The bridge C-O-C antisymmetric stretching vibration is distinguishable for the vibration located at 1161 cm^{-1}, and the peak at 1106 cm^{-1} derives from the antisymmetric ring stretching. Peaks at 1056 cm^{-1} and 1034 cm^{-1} relate to the -C-O stretching mode; the vibration located at 896 cm^{-1} is characteristic of the β-1,4 glycosidic linkage [9],[10].

The absence of vibrational modes of constituents of the cuticle and the outermost layer of the cotton fiber (i.e., waxes, pectins, and proteins) suggests that analyzed fabrics were subjected to a scouring process [9],[11].

The spectrum in Figure 3b shows very distinctive infrared signatures of silk components, which were similar between different fabrics. The Amide group of fibroin, the main protein of silk, presents vibrational modes sensitive to β - sheet, α-helical, and random coil protein conformations. Spectral deconvolutions of the Amide I absorption region show, for all analyzed fibers, three contributions attributed to these different secondary structures. Specifically, IR signals at 1620 cm^{-1} and 1698 cm^{-1} referred to β-sheet [12] and antiparallel β-sheet [13] secondary structures, respectively, while the third contribution at ca. 1644 cm^{-1} is typical of random coil (non-ordered) conformations [13]. The signal detected at 1517 cm^{-1} is characteristic of the Amide II vibrational mode (-N-H bending and C-N bending).

Peaks in the spectral zone 1340-1456 cm^{-1} are associated with aminoacid vibration modes [14]. For instance, the most intense peak at 1446 cm^{-1} or the absorption at 1398 cm^{-1} are typical of the $-CH_2$ and $-CH_3$ or $-CH_2$ and -OH bending in alanine or serine residues, respectively [15]. The vibration at 1164 cm^{-1} instead characterizes the -C-N stretching in tyrosine residues [16]. The Amide III vibration mode (-C-N stretching and -N-H bending) is at 1260 cm^{-1} or 1230 cm^{-1} for diverse analyzed fibers, indicating the occurrence of β-sheet or random coil protein secondary structures, respectively [17].

Overall, cotton, hemp, and silk have been identified as the principal materials for all the investigated samples, yet knowing the microstructure of these fabrics, which, in turn, could reflect their conservation conditions, is essential to determine the appropriate conservative approach. Thus,

silk proteins' FTIR contributions were more deeply analyzed to assess the conservative state of silk fibers and their crystallinity degree, which is a crucial indicator of silk aging. In this regard, silk fibroin consists mainly of a hexapeptide repeated pattern (-Gly-Ala-Gly-Ala-Gly-Ser-), forming antiparallel β-sheet crystallites. An amorphous matrix of residues with bulky and polar side chains surrounds these crystallites. Amorphous areas are more prone to degradation, which derives from contact with oxygen or water. As degradation proceeds, crystallites are also damaged and lose their alignment. Consequently, silk textiles lose their physical and chemical properties, such as elasticity and mechanical strength [18]. Silk fibers' crystallinity index (CI) was calculated from ATR-FTIR spectra comparing the intensities of two vibrational modes of Amide III. The absorption intensity associated with a β-sheet structure (1263 cm^{-1}) was divided by that of random-coil conformation (1230 cm^{-1}) [19],[20] (Table 2). The intensity ratio I_{1260}/I_{1230} was calculated after correcting for a local baseline drawn from 1300 cm^{-1} to 1180 cm^{-1}.

Table 2. Crystallinity index values for some threads of the analyzed fabrics.

Sample	I_{1263}[a]	I_{1230}[a]	CI	Crystallinity degree (%)[c]
INV251 light green warp	0.0394	0.0690	0.571	36.3
INV251 dark green warp	0.0435	0.0778	0.558	35.8
INV253D warp	0.0083	0.0204	0.407	28.9
INV253E green warp	0.0264	0.0500	0.528	34.5
INV253E blue weft	0.0183	0.0342	0.536	34.9
INV253G blue weft	0.0290	0.0529	0.548	35.4
INV253G red warp	0.0314	0.0582	0.540	35.1
INV253F green warp	0.0144	0.0279	0.517	34.1
INV253A brown warp	0.0145	0.0279	0.519	34.2
INV253B orange warp	0.0275	0.0478	0.576	36.5
INV254F green warp	0.0187	0.0384	0.487	32.8
INV254E warp	0.0252	0.0555	0.455	31.3
INV254A green selvedge	0.0292	0.0503	0.580	36.7
INV254B blue weft	0.0153	0.0247	0.620	38.3
INV254F gold weft	0.0180	0.0271	0.664	39.9

[a] I_{1263} and I_{1230} are intensity values at 1263 cm^{-1} and 1230 cm^{-1}

[b] $CI=I_{1263}/I_{1230}$.

[c] Crystallinity degree (%) = $I_{1263}/(I_{1263}+ I_{1230})$

All the analyzed silk threads show a similar crystallinity degree, which is lower than unaged silk [19]. This finding accounts for the delicate crystalline structure of silk, which is easily affected by deterioration agents over time.

To deepen information concerning the conservation status of the above textiles, the evaluation of tyrosine content was performed. Indeed, sunlight oxidizes this aromatic aminoacid into yellow chromophores responsible for the photo-yellowing followed by photo-tendering of silk textile products [19]. The signal at 1160 cm^{-1} is attributed to the phenol residues of tyrosine. The area ratio of the peak at 1160 cm^{-1} to the 1621 cm^{-1} peak, used as an internal standard, reflects the tyrosine content (Table 3).

The area of the peak at 1160 cm^{-1} was calculated considering a local baseline between 1185 cm^{-1} and 1140 cm^{-1}; the area of the contribution at 1620 cm^{-1} was obtained through spectral deconvolutions of the Amide I spectral region (1730 cm^{-1}-1570 cm^{-1}).

All analyzed wires show a very low tyrosine content compared to that reported in the literature for unaged silk [19]. This finding, together with the low crystallinity index, are indicative of an advanced aging degree. The sample INV253D warp is the most aged, as indicated by its crystallinity value and tyrosine content.

Table 3. Area ratios indicative of the tyrosine content.

Sample	A_{1169}[a]	A_{1620}[a]	A_{1169}/ A_{1620}
INV251 light green warp	0.690	11.271	0.061
INV251 dark green warp	0.721	12.046	0.060
INV253D warp	0.102	5.572	0.018
INV253E green warp	0.439	7.373	0.060
INV253E blue weft	0.279	5.667	0.049
INV253G blue weft	0.539	9.308	0.058
INV253G red warp	0.505	7.343	0.069

INV253F green warp	0.264	3.655	0.072
INV253A brown warp	0.309	3.389	0.091
INV253B orange warp	0.604	6.973	0.087
INV254F green warp	0.462	4.910	0.094
INV254E warp	0.559	6.062	0.092
INV254A green selvedge	0.505	8.800	0.057
INV254B blue weft	0.547	3.075	0.178
INV254F gold weft	0.409	5.481	0.075

[a] A_{1169} and A_{1620} are area values of peaks at 1169 cm^{-1} and 1620 cm^{1}

Evaluating the sericin content of silk textiles is pivotal to designing a correct intervention for cleaning and preservation. Indeed, knowing the amount of water-soluble sericin that remained after the silk degumming procedure [21] could be essential for curators to choose the correct cleaning solvent.

Unlike fibroin, sericin has an amorphous structure and exhibits a specific vibrational mode that correlates with a random coil secondary structure.

For a quantitative evaluation of the sericin content, the peak at 1400 cm^{-1}, indicative of aminoacid side chains in sericin, is compared to the fibroin-related one at 1444 cm^{-1} (Table 4) [21]. The intensity ratio I_{1400}/I_{1444} was calculated after correcting for a local baseline drawn from 1470 and 1350 cm^{-1}.

Table 4. Intensity ratios indicatives of sericin content in some threads of the analyzed fabrics.

Sample	I_{1400}[a]	I_{1444}[a]	I_{1400}/I_{1444}
INV251 light green warp	0.0239	0.0718	0.332
INV251 dark green warp	0.0266	0.0794	0.335
INV253D warp	0.0299	0.0088	3.414
INV253E green warp	0.0193	0.0486	0.397
INV253E blue weft	0.0266	0.0356	0.747
INV253G blue weft	0.0212	0.0607	0.350
INV253G red warp	0.0243	0.0590	0.412
INV253F green warp	0.0073	0.0242	0.299
INV253A brown warp	0.0089	0.0246	0.361
INV253B orange warp	0.0523	0.0586	0.891
INV254F green warp	0.0173	0.0335	0.517
INV254E warp	0.0184	0.0242	0.763
INV254A green selvedge	0.0205	0.0558	0.367
INV254B blue weft	0.0494	0.0423	1.168
INV254F gold weft	0.0141	0.0304	0.464

[a] I_{1400} and I_{1444} are intensity values at 1400 cm^{-1} and 1444 cm^{-1}

For most samples, the calculated ratios are typical of degummed silk and consistent with those reported by Zhang et al. [21]. The sample INV253D warp with a very high amount of sericin has the lowest crystallinity degree. Notwithstanding, a direct correlation between CI and sericin content is not straightforward. Indeed, the comparison among CI and tyrosine content indicates a poor conservation status for sample INV253D, while for all other fibers, the parameter values suggest a better conservation status. This aspect deserves to be deepened further.

In other analyzed threads (i.e., INV253E blue weft, INV253B orange warp, INV254F green warp, INV254E warp, INV254B blue weft), the sericin content is not particularly high, likely due to the partial silk degumming process.

Finally, ATR-FTIR spectra do not show typical vibrational modes of organic dyes. This outcome likely traces back to the low quantity of organic dyes used for these textiles and the intense cotton and silk signals masking dyes' contributions.

IV. CONCLUSIONS

In the context of a restorative-conservative intervention, the physical-chemical characterization of unique Japanese fabrics clarified their nature. The presence of cotton, hemp, and silk can be linked to production between the 19th and 20th centuries. It is precisely in this period that, in addition to the oldest processing of silk and hemp, cotton processing increases also. The study of the crystallinity degree alongside sericin and tyrosin content, obtained from ATR-FTIR spectra of silk, allowed us to evaluate the conservative state of the materials.

Furthermore, metals such as gold and silver are consistent with metal lamination.

This work is only a preliminary analysis since the peculiarities and differences between the fabrics, especially in terms of elemental composition, deserve to be deepened in further investigations.

V. REFERENCES

[1] R. Alcock, "Lacquer ware, wallpapers, textile fabrics, and embroidery". Art and Art Industries in Japan,Virtue & Co, London, 1878.

[2] W. Wailliez, "Japanese leather paper or Kinkarakawagami: an overview from the 17th century to the Japonist hangings by Rottmann & Co. Wallpap". Hist. Rev., vol.7, 2015, pp.60–65

[3] M.A. Spadaro, "O'Tama e Vincenzo Ragusa. Echi di Giappone in Italia", Kalós, Palermo, Italy 2008

[4] E. Piacenza, A. Presentato, F. Di Salvo, R. Alduina, V.

Ferrara, V. Minore, A. Giannusa, G. Sancataldo, D.F. Chillura Martino, “A combined physical–chemical and microbiological approach to unveil the fabrication, provenance, and state of conservation of the Kinkarakawa-gami art”. SciReport 2020, vol.10, 16072.

[5] G. Chirco, E.C. Portale, E. Caponetti, V. Renda, D.F. Chilliura Martino “Investigation on four centuripe vases (late 3rd-2nd cent. B.C.) by portable X-ray fluorescence and total reflectance-FTIR”, Journal of Cultural Heritage, vol.48, 2021, pp.326-335

[6] G. Chirco, M. De Cesare, G. Chiari, S. Maaß, M.L. Saladino, D.F. Chillura Martino, “Archaeometric study of execution techniques of white Attic vases: the case of Perseus crater in Agrigento”, RCS Advances, vol.12, 2022, pp.4526-4535

[7] R. M. Rousseau, “Fundamental algorithm between concentration and intensity in XRF analysis 2—practical application”, X-Ray Spectrometry, vol.13, No.3, 1984, pp.121-125

[8] R. Tertian, “Mathematical matrix correction procedures for X-ray fluorescence analysis. A critical survey”, X-Ray Spectrometry, vol.15, No.3, 1986, pp.177-190

[9] C. Chinkap, L. Myunghee, C. Eun Kyung, “Characterization of cotton fabric scouring by FT-IR ATR spectroscopy”, Carbohydrate Polymers, vol.58, No.4, 2004, pp.417–420.

[10] N. Abidi, L. Cabrales, E. Hequet, “Fourier transform infrared spectroscopic approach to the study of the secondary cell wall development in cotton fiber”, Cellulose, vol.17, 2010, pp.309-320.

[11] E.K. Choe, L. Myunghee, K.S. Park, C. Chung, “Characterization of cotton fabric scouring by Fourier transform-infrared attenuated total reflectance spectroscopy, gas chromatography-mass spectrometry and water absorption measurements”, Textile Research Journal, vol.89, No.12, 2018, pp.2305-2315

[12] A. Vasconcelos, G. Freddi, A. Cavaco-Paulo, “Biodegradable materials based on silk fibroin and keratin”, Biomacromolecules, vol. 9, No. 4, 2008, pp. 1299-1305.

[13] E. Bramanti, D. Catalano, C. Forte, M. Giovanneschi, M. Masetti, C.A. Veracini, “Solid state 13C NMR and FT-IR spectroscopy of the cocoon silk of two common spiders”, Spectrochimica Acta Part A, vol.62, No.1-3, 2005, pp.105-111

[14] A. Barth, “The infrared absorption of amino acid side chains”, Progress in Biophysics and Molecular Biology, vol.74, No.3-5, 2000, pp.141-173

[15] M. Boulet-Audet, F. Vollrath, C. Holland, “Identification and Classification of Silks Using Infrared Spectroscopy”, Journal of Experimental Biology, vol.218, No.19, 2015, pp.3138–3149.

[16] M.A. Koperska, D. Pawcenis, J. Bagniuk, M.M. Zaitz, M. Missori, T. Lohewski, “Degradation markers of fibroin in silk through infrared spectroscopy”, Polymer Degradation and Stability, vol.105, No.2014, 2014, pp.185-196

[17] O. Marinicas, M. Giurginca, “Conservation-restoration of textile materials from Romanian medieval art collections”, Rev. Chim., vol.60, No.9, 2009, pp.9-14

[18] P. Garside, P. Wyeth, “Crystallinity and degradation of silk: correlations between analytical signatures and physical condition on ageing”, Applied Physic A, vol. 89, 2007, pp.871-876

[19] J. Shao, J. Zheng, J. Liu, C.M. Carr, “Fourier Transform Raman and Fourier Transform Infrared Spectroscopy Studies of Silk Fibroin”, Journal of Applied Polymer Science, vol.96, No.6, 2005, pp.1999-2004

[20] I.C. Um, H.Y. Kweon, Y. H. Park, S. Hudson, “Structural characteristics and properties of the regenerated silk fibroin prepared from formic acid”, International Journal of Biological Macromolecules, vol.29, No.2, 2001, pp.91-97

[21] X.M. Zhang, P. Wyeth, “Using FTIR spectroscopy to detect sericin on historic silk”, Science China Chemistry, vol.53, No.3, 2010, pp.626-631